Published in final edited form as:
Curr Biol. 2009 December 15; 19(23): 2043–2049. doi:10.1016/j.cub.2009.10.050.

Clustering of centralspindlin is essential for its accumulation to the central spindle and the midbody

Andrea Hutterer[1], **Michael Glotzer**[2,*], and **Masanori Mishima**[1,*]

[1]Wellcome/CRUK Gurdon Institute, University of Cambridge, UK

[2]Department of Molecular Genetics and Cell Biology, University of Chicago, IL

Summary

Cytokinesis in animal cells requires the central spindle and midbody which contain prominent microtubule bundles [1]. Centralspindlin, a heterotetrameric complex consisting of Kinesin-6 and RhoGAP (Rho-family GTPase-activating protein) subunits, is essential for the formation of these structures [2]. Centralspindlin becomes precisely localized to the central spindle where it promotes the equatorial recruitment of important cytokinetic regulators. These include ECT2, the activator of the small GTPase RhoA, which controls cleavage furrow formation and ingression [3-6]. Centralspindlin's own RhoGAP domain also contributes to furrow ingression [7-10]. Finally, centralspindlin facilitates recruitment of the chromosome passenger complex [7, 8] and factors that control abscission [11, 12]. Despite the importance of localized accumulation of centralspindlin, the mechanism by which this motor protein complex suddenly concentrates to the centre of interpolar microtubule bundles during anaphase is unclear. Here, we show that centralspindlin travels along central spindle microtubules as higher-order clusters. Clustering of centralspindlin is critical for microtubule bundling and motility along microtubules in vitro, and for midbody formation in vivo. These data support a positive feedback loop of centralspindlin clustering and microtubule organization that may underlie its distinctive localization during cytokinesis.

Results and Discussion

Centralspindlin moves along microtubules as clusters and stably accumulates at the midzone

Centralspindlin is a stable tetramer formed by a dimer of a RhoGAP HsCYK-4 (aka RACGAP1/HsMgcRacGAP, *C. elegans* CYK-4, *Drosophila* RacGAP50C/Tumbleweed) and a Kinesin-6 dimer MKLP1 (aka KIF23, *C. elegans* ZEN-4, *Drosophila* Pavarotti). Although the motor activity of MKLP1 is essential for accumulation of centralspindlin to the centre of the midbody [13], the mechanism for its specific accumulation is unknown. To gain insight into this process, we observed GFP-tagged HsCYK-4 [14], expressed in HeLa cells by total internal reflection fluorescence (TIRF) microscopy. The central spindle was brought within reach of TIRF illumination by overlaying the cells with an agarose slab (Figure. 1A). This enabled us to observe particles of HsCYK-4-GFP moving along tracks that are likely to be spindle midzone microtubules (Figure 1B and Supplementary Movie 1). In six early anaphase cells, 74 tracks were detected on which 120 centralspindlin particles were observed to move for longer than 1 s with an average velocity of 312 +/− 22 nm/s. Examples of moving particles are shown in the kymographs in Figure 1C. The signal of most moving particles exhibited gradual rather than stepwise decay (Figure 1D), indicating that each

*To whom correspondence should be addressed. m.mishima@gurdon.cam.ac.uk (M. M.); mglotzer@uchicago.edu (M. G.) .

Europe PMC Funders Author Manuscripts

particle contains multiple GFP moieties and therefore likely reflects multiple centralspindlin molecules in a cluster.

We next assessed whether centralspindlin, once concentrated, is stable at the central spindle or whether it exhibits dynamic exchange by fluorescence recovery after photobleaching (FRAP). During metaphase, when centralspindlin is diffuse throughout the cytoplasm, recovery of bleached HsCYK-4-GFP was rapid and complete with a half-time of less than 5 s (Figure 1E). However, during anaphase, the recovery of midzone-localized HsCYK-4-GFP was very limited (less than 10% in 2 min) (Figure 1E). The stable accumulation of centralspindlin to anaphase microtubules is in stark contrast to the rapid recovery exhibited by other microtubulelocalized motor proteins: Kinesin-5 localized at the spindle midzone turns over with a half-time of less than 30 s [15, 16] and microtubule bound Kinesin-1 at the periphery of interphase cells turns over with a half-time of 16 s [17]. Simple motor-microtubule interactions are therefore insufficient to explain how centralspindlin stably associates with the spindle midzone.

The stable accumulation of centralspindlin at the spindle midzone and its tendency to assemble into motile clusters is consistent with previously characterised biochemical properties of centralspindlin. Neither centralspindlin in *C. elegans* embryonic lysates nor recombinant *C. elegans* centralspindlin expressed in insect cells is fully soluble in low ionic strength solutions [2]. Likewise, centralspindlin in HeLa cell lysates also becomes less soluble during cytokinesis (Figure 1F) and purified human centralspindlin can be partially sedimented by centrifugation (Figure 1G). In a buffer with physiological salt concentrations, the soluble pool of ZEN-4 (*C. elegans* Kinesin-6) plateaus at ~15 μg/ml (Figure 2A, B 1-775), which is comparable to its concentration in embryos (Figure S2). This indicates that the clustering could occur under physiological conditions, which would be further enhanced by concentration at sites such as the spindle midzone. Importantly, this effect is reversible (Figure 2C) and therefore cannot be due to irreversible aggregation. While protein insolubility could be caused by incomplete folding or absence of a critical binding partner, there are precedents for physiological clustering of proteins. Myosin-II, another essential cytokinesis motor protein, shows similar salt-sensitive insolubility, reflecting its ability to form a large assembly that is critical for its function [18, 19]. We hypothesised that the low solubility of centralspindlin in vitro might reflect its in vivo ability to assemble into multimeric clusters that travel along the midzone microtubules. Clustering of centralspindlin could contribute to its stable accumulation to the spindle midzone because the increased avidity induced by clustering would stabilize the association with microtubules.

A short element in Kinesin-6 is specifically required for clustering

To test this hypothesis, we sought to identify a separation-of-function mutation. A derivative of centralspindlin that is clustering defective but retains all other activities would enable us to assess the significance of clustering for its in vitro and in vivo functions. For these studies, we focused on *C. elegans* centralspindlin, so that we could combine in vitro biochemical and biophysical analyses with in vivo genetic studies. To assay for a mutant defective for clustering, we used the sedimentation assay. ZEN-4 exhibits low solubility in the presence or absence of CYK-4 [2]. Deletions from the C-terminus of ZEN-4 revealed that the C-terminal domain of ZEN-4 is dispensable for clustering (Figure 2C, ZEN-4 (1-601) (Z601)). Remarkably, removal of 16 additional amino acids rendered ZEN-4 completely soluble even under low salt concentrations (Figure 2D and S3A, ZEN-4 (1-585) (Z585)), indicating that the region between residues 586-601 of ZEN-4 is critical for clustering. Deletion of this ‘clustering element’, in an otherwise full-length ZEN-4 construct greatly increased its solubility (Figure 2A and B). Deletion of this region did not affect the other known activities of ZEN-4, binding to CYK-4 (Figures 2E and S3B) and homo-

dimerization [20] (Figure S3C). These results indicate that the clustering of centralspindlin is separable from other functional domains of ZEN-4 (Figure 2F and S3D).

Clustering of centralspindlin is essential for productive interactions with microtubules

microtubulesTo address how clustering contributes to centralspindlin function, we compared the behaviour of ZEN-4 derivatives with or without the clustering element in in vitro and in vivo assays. Firstly, we examined their microtubule-bundling activities. A complex of clustering competent Z601 and CYK-4 (1-232) showed strong microtubule bundling activity (Figure 2G) [20]. In contrast, a complex of the clustering defective Z585 and CYK-4 (1-232) exhibited significantly reduced microtubule-bundling activity as revealed by the presence of many unbundled microtubules (Figure 2G). This suggests that clustering contributes to efficient microtubule bundling.

Secondly, to examine whether clustering affects the function of ZEN-4 as a microtubule motor protein, we observed the motility of GFP-tagged ZEN-4 proteins along surface-immobilized microtubules by TIRF microscopy. As plus-end directed motors [21], both Z585 and Z601 tagged with GFP (Z585GFP and Z601GFP, respectively) support gliding of microtubules when immobilized on coverglass surface (data not shown). Like the untagged proteins, both of them are dimers in the presence of high salt (Figure S3E) and Z601GFP assembles into large clusters under low salt conditions while Z585GFP fails to do so (Figure S3F). At near-physiological concentration of the motors (9 μg/ml), too high for observation of single molecules, both proteins associated with the entire length of microtubules (Figure 3A). Z601GFP, but not Z585GFP, showed prominent accumulation at one of the two ends of the microtubules, which was identified as the plus-end with polarity-marked microtubules (Figure S4A). This suggests that clustering promotes accumulation of ZEN-4 at microtubule plus ends.

When the motors were further diluted (135 ng/ml), continuous movement of individual Z601GFP particles along microtubules became visible (for up to 10 s) (Figure 3B and C, Supplementary Video 2). A subset of the particles travelled to the end of the microtubule and remained associated with the plus end (Figure 3C arrow head, Figure S4B). In contrast, the majority of Z585GFP particles attached briefly to microtubules and did not move continuously, but rather diffused on the microtubule before dissociating (Figure 3F, G, H, Supplementary Video 3). Although the majority of particles disappeared in a single step either by detachment from microtubules or by photobleaching, some Z601GFP particles photobleached in two-, three-, four- or even more steps of roughly equal heights, indicating that these particles contained multiple ZEN-4-GFP polypeptides (Figure 3D).

To understand the effect of clustering on the motile behaviour, we estimated the number of ZEN-4 dimers in each particle that moves along a microtubule. We used the initial intensity of each particle as an estimate of its degree of clustering since the number of photobleaching steps can not be counted for particles with short association times. Analysis of dimeric constructs (Z585GFP and a Kinesin-1 dimer (K432GFP)) revealed that 40 to 50% of GFP moieties are fluorescently active in our samples (Figure 3 F-H and L-N, Figure S5A). Therefore, the fluorescence intensity (as well as photobleaching step numbers) is not directly proportional to the number of GFP-fused polypeptides in a particle but would rather follow broad probabilistic distributions (Figure 3P). For example, Z601GFP particles whose intensity (I) is 2-fold higher than that of a single GFP (I_{GFP}), would include not only dimers but also some larger oligomers with only two fluorescently active GFP moieties. At the concentration required for visualizing individual particles, the majority of Z601GFP clusters dissociated into dim particles ($I/I_{GFP} < 2.5$) (Figure 3E), reflecting the reversibility of clustering (Figure 2C). However, some Z601GFP particles remained as brighter clusters and these particles moved continuously along a microtubule for longer periods (correlation

coefficient = 0.59 for particles with association time longer than 2 s) (Figure 3E). The effect of clustering on the processivity of motility was striking. Oligomeric clusters of Z601GFP, $I/I_{GFP} \geq 2.5$, moved continuously along microtubules for longer than 4 s while Z585 dimers, $I/I_{GFP} < 2.5$, detached from microtubules in 0.3 s (Figures 3O and S6G). The short association time of Z585GFP is not due to rapid bleaching as it is ~15 times shorter than the average bleaching time for GFP (Figure S5B). Although clustering caused a moderate reduction in the velocity, it increased run length significantly (> 5-fold) (Figure 3O). Thus, clustering dramatically increases overall transport efficiency along microtubules.

To confirm that clustering of ZEN-4 is sufficient for continuous motility, we tested whether artificial oligomerization of Z585GFP can restore its stable motility (Figure 3I-K). We used avidin-mediated cross-linking through a 15 amino acid C-terminal tag that is biotinylated in *E. coli* [22]. Remarkably, avidin-induced oligomeric clusters containing multiple dimers that exhibited continuous movement along microtubules (Figure 3K, Supplementary Video 4). Similar to Z601GFP, Z585GFP clustered by avidin also accumulated at microtubule plus ends (Figure 3I arrow head), indicating that clustering is both necessary and sufficient for highly stable motility of ZEN-4, which facilitates its accumulation to microtubule plus ends.

Clustering of centralspindlin is essential for its accumulation to the midbody and completion of cytokinesis

Finally, to determine whether clustering is important for the in vivo function of centralspindlin, we compared the ability of a wild-type *zen-4* transgene and a mutant transgene defective for clustering to rescue the recessive lethality caused by a null allele of *zen-4(w35)* [23]. For this purpose, we generated multiple, independent lines that harbour *zen-4::GFP* or *zen-4Δ586-603::GFP* as stably integrated, low copy transgenes [24]. All *zen-4::GFP* transgenic lines efficiently rescued *zen-4* null homozygous animals (30 to 85%) (Figure 4A). Rescued animals were fertile and could be stably maintained. In clear contrast, the *zen-4Δ586-603::GFP* transgenes failed to efficiently rescue the *zen-4* null allele (no rescue in 3 lines and 12% in one line). Moreover, none of the animals rescued by the mutant transgene could produce viable progeny. Thus the clustering element is essential for the in vivo function of centralspindlin.

We were able to obtain embryos from homozygous *zen-4* null hermaphrodites rescued by both types of transgenes with which we could assay the behaviour of the ZEN-4::GFP fusion proteins in the absence of endogenous wild-type ZEN-4 protein. As expected from the high level of rescue efficiency, most embryos expressing ZEN-4 WT::GFP successfully completed cytokinesis (8/10). As previously reported, ZEN-4 WT::GFP began to accumulate on the central spindle in anaphase and strongly concentrated at the midbody (Figure 4B). It remained highly concentrated in the midbody for at least 20 minutes after the completion of furrowing. In contrast, ZEN-4Δ586-603::GFP did not strongly accumulate to the central spindle and midbody. We detected weak and transient signals of the mutant ZEN-4 at the central spindle in most embryos (10/15 embryos, Figure 4B arrow). However, these signals dispersed within 1-2 minutes and stable accumulation to the midbody was not observed. As a consequence, all embryos expressing mutant ZEN-4 failed to complete cytokinesis (15/15). The ability of the clustering element to promote both microtubule association and continuous motility (Figure 3) provides a simple explanation for this phenotype. Centralspindlin clustering appears crucial for its discrete and stable accumulation to the central spindle and the midbody.

A positive feedback loop of centralspindlin clustering and microtubule bundling could drive centralspindlin accumulation

This study demonstrates the importance of the higher-order clustering of a kinesin superfamily molecule in its cellular functions. It extends previous theoretical predictions and in vitro observations that clustering of low-processivity motors increases their run lengths [25-29]. There are notable similarities between the assembly properties of ZEN-4 and the actin based motor myosin II, suggesting that oligomerization may contribute to motility in diverse motors and biological contexts. Motility as clusters leads to the accumulation of centralspindlin to the microtubule plus ends (Figure 5A). This could explain the recently reported accumulation of centralspindlin to the plus-ends of equatorial astral microtubules [30, 31]. Clustering of centralspindlin also facilitates microtubule bundling. Both plus-end accumulation and microtubule-bundling would increase the local concentration of centralspindlin, which in turn would enhance cluster formation and promote interactions with microtubules, thereby closing a positive feedback loop (Figure 5B).

This model has important implications for the mechanism of rapid and intense accumulation of centralspindlin during cytokinesis since positive feedback in general can accelerate the response to a regulatory switch and amplify spatial differences. Activation of centralspindlin at anaphase onset might trigger the start of this feedback loop by increasing centralspindlin's affinity for microtubules [32, 33]. This feedback loop is predicted to be sensitive to the organization as well as the stability of microtubule arrays. An astral array of microtubules with minus-ends at the centre as found in mitotic asters would not take full advantage of this positive feedback loop since the outward movement of centralspindlin along microtubules would result in a decrease in its local concentration. In an anaphase cell, however, this positive feedback loop would be facilitated in the equatorial region, where two groups of microtubules with opposite polarities meet (Figure 5C). This would explain how centralspindlin preferentially accumulates to the spindle midzone as compared to the surrounding astral microtubules. Selective stabilization of a subset of microtubules by chromosomes [34] or cortical contractility [35] might provide other means of engaging this feedback loop.

Supplementary Material

Refer to Web version on PubMed Central for supplementary material.

Acknowledgments

We thank J. Mason, P. Das, R. Andrew, A. Sossick and T. Davies for technical assistance; J. Ahringer and E. Miska for advice on *C. elegans* experiments; J. Howard, S. Diez, Y. Okada and M. Savoian for helpful discussions; and J. Raff, J. Pines, M. Douglas for critical comments on the manuscript. MM and MG collaborated on experimental design, data interpretation and writing the manuscript. MM and AH performed the experiments. This research was supported by Cancer Research UK programme grant C19769/A6356 and equipment grant C19769/A7164 (M. M.), Human Frontier Science Program and EMBO (A. H.) and National Institute of General Medical Sciences (NIGMS) R01 GM074743 (M. G.).

References

1. Glotzer M. The 3Ms of central spindle assembly: microtubules, motors and MAPs. Nat Rev Mol Cell Biol. 2009; 10:9–20. [PubMed: 19197328]
2. Mishima M, Kaitna S, Glotzer M. Central spindle assembly and cytokinesis require a kinesin-like protein/RhoGAP complex with microtubule bundling activity. Dev Cell. 2002; 2:41–54. [PubMed: 11782313]

3. Somers WG, Saint R. A RhoGEF and Rho family GTPaseactivating protein complex links the contractile ring to cortical microtubules at the onset of cytokinesis. Dev Cell. 2003; 4:29–39. [PubMed: 12530961]
4. Yüce O, Piekny A, Glotzer M. An ECT2-centralspindlin complex regulates the localization and function of RhoA. J Cell Biol. 2005; 170:571–582. [PubMed: 16103226]
5. Kamijo K, Ohara N, Abe M, Uchimura T, Hosoya H, Lee JS, Miki T. Dissecting the role of Rho-mediated signaling in contractile ring formation. Mol Biol Cell. 2005; 17:43–55. [PubMed: 16236794]
6. Zhao WM, Fang G. MgcRacGAP controls the assembly of the contractile ring and the initiation of cytokinesis. Proc Natl Acad Sci U S A. 2005; 102:13158–13163. [PubMed: 16129829]
7. Jantsch-Plunger V, Gonczy P, Romano A, Schnabel H, Hamill D, Schnabel R, Hyman AA, Glotzer M. CYK-4: A Rho family gtpase activating protein (GAP) required for central spindle formation and cytokinesis. J Cell Biol. 2000; 149:1391–1404. [PubMed: 10871280]
8. Zavortink M, Contreras N, Addy T, Bejsovec A, Saint R. Tum/RacGAP50C provides a critical link between anaphase microtubules and the assembly of the contractile ring in Drosophila melanogaster. J Cell Sci. 2005; 118:5381–5392. [PubMed: 16280552]
9. Canman JC, Lewellyn L, Laband K, Smerdon SJ, Desai A, Bowerman B, Oegema K. Inhibition of Rac by the GAP activity of centralspindlin is essential for cytokinesis. Science. 2008; 322:1543–1546. [PubMed: 19056985]
10. Miller AL, Bement WM. Regulation of cytokinesis by Rho GTPase flux. Nat Cell Biol. 2009; 11:71–77. [PubMed: 19060892]
11. Gromley A, Yeaman C, Rosa J, Redick S, Chen CT, Mirabelle S, Guha M, Sillibourne J, Doxsey SJ. Centriolin anchoring of exocyst and SNARE Complexes at the midbody is required for secretory-vesiclemediated abscission. Cell. 2005; 123:75–87. [PubMed: 16213214]
12. Zhao WM, Seki A, Fang G. Cep55, a microtubule-bundling protein, associates with centralspindlin to control the midbody integrity and cell abscission during cytokinesis. Mol Biol Cell. 2006; 17:3881–3896. [PubMed: 16790497]
13. Matuliene J, Kuriyama R. Kinesin-like protein CHO1 is required for the formation of midbody matrix and the completion of cytokinesis in mammalian cells. Mol Biol Cell. 2002; 13:1832–1845. [PubMed: 12058052]
14. Wolfe BA, Takaki T, Petronczki M, Glotzer M. Polo-like kinase 1 directs assembly of the HsCyk-4 RhoGAP/Ect2 RhoGEF complex to initiate cleavage furrow formation. PLoS Biol. 2009; 7:e1000110. [PubMed: 19468300]
15. Cheerambathur DK, Brust-Mascher I, Civelekoglu-Scholey G, Scholey JM. Dynamic partitioning of mitotic kinesin-5 cross-linkers between microtubule-bound and freely diffusing states. J Cell Biol. 2008; 182:429–436. [PubMed: 18678711]
16. Uteng M, Hentrich C, Miura K, Bieling P, Surrey T. Poleward transport of Eg5 by dynein-dynactin in Xenopus laevis egg extract spindles. J Cell Biol. 2008; 182:715–726. [PubMed: 18710923]
17. Dunn S, Morrison EE, Liverpool TB, Molina-París C, Cross RA, Alonso MC, Peckham M. Differential trafficking of Kif5c on tyrosinated and detyrosinated microtubules in live cells. J Cell Sci. 2008; 12:1085–1095. [PubMed: 18334549]
18. Niederman R, Pollard TD. Human platelet myosin. II. In vitro assembly and structure of myosin filaments. J Cell Biol. 1975; 67:72–92. [PubMed: 240861]
19. Mabuchi I. Myosin from starfish egg: properties and interaction with actin. J Mol Biol. 1976; 1976:569–582. [PubMed: 3657]
20. Pavicic-Kaltenbrunner V, Mishima M, Glotzer M. Cooperative Assembly of CYK-4/MgcRacGAP and ZEN-4/MKLP1 to Form the Centralspindlin Complex. Mol Biol Cell. 2007; 18:4992–5003. [PubMed: 17942600]
21. Nislow C, Lombillo VA, Kuriyama R, McIntosh JR. A plus-end-directed motor enzyme that moves antiparallel microtubules in vitro localizes to the interzone of mitotic spindles. Nature. 1992; 359:480–482. [PubMed: 1406965]
22. Beckett D, Kovaleva E, Schatz PJ. A minimal peptide substrate in biotin holoenzyme synthetase-catalyzed biotinylation. Protein Sci. 1999; 8:921–929. [PubMed: 10211839]

23. Raich WB, Moran AN, Rothman JH, Hardin J. Cytokinesis and midzone microtubule organization in Caenorhabditis elegans require the kinesin-like protein ZEN-4. Mol Biol Cell. 1998; 9:2037–2049. [PubMed: 9693365]
24. Praitis V, Casey E, Collar D, Austin J. Creation of low-copy integrated transgenic lines in Caenorhabditis elegans. Genetics. 2001; 157:1217–1226. [PubMed: 11238406]
25. Howard J. Molecular motors: structural adaptations to cellular functions. Nature. 1997; 389:561–567. [PubMed: 9335494]
26. Tomishige M, Klopfenstein DR, Vale RD. Conversion of Unc104/KIF1A kinesin into a processive motor after dimerization. Science. 2002; 297:2263–2267. [PubMed: 12351789]
27. Klumpp S, Lipowsky R. Cooperative cargo transport by several molecular motors. Proc Natl Acad Sci U S A. 2005; 102:17284–17289. [PubMed: 16287974]
28. Furuta K, Edamatsu M, Maeda Y, Toyoshima YY. Diffusion and directed movement: In vitro motile properties of fission yeast kinesin-14 Pkl1. J Biol Chem. 2008
29. Surrey T, Nedelec F, Leibler S, Karsenti E. Physical properties determining self-organization of motors and microtubules. Science. 2001; 292:1167–1171. [PubMed: 11349149]
30. D'Avino PP, Savoian MS, Capalbo L, Glover DM. RacGAP50C is sufficient to signal cleavage furrow formation during cytokinesis. J Cell Sci. 2006; 118:1549–1558.
31. Nishimura Y, Yonemura S. Centralspindlin regulates ECT2 and RhoA accumulation at the equatorial cortex during cytokinesis. J Cell Sci. 2006; 119:104–114. [PubMed: 16352658]
32. Mishima M, Pavicic V, Grüneberg U, Nigg EA, Glotzer M. Cell cycle regulation of central spindle assembly. Nature. 2004; 430:908–913. [PubMed: 15282614]
33. Goshima G, Vale RD. Cell cycle-dependent dynamics and regulation of mitotic kinesins in Drosophila S2 cells. Mol Biol Cell. 2005; 16:3896–3907. [PubMed: 15958489]
34. Canman JC, Cameron LA, Maddox PS, Straight A, Tirnauer JS, Mitchison TJ, Fang G, Kapoor TM, Salmon ED. Determining the position of the cell division plane. Nature. 2003; 424:1074–1078. [PubMed: 12904818]
35. Hu CK, Coughlin M, Field CM, Mitchison TJ. Cell polarization during monopolar cytokinesis. J Cell Biol. 2008; 181:195–202. [PubMed: 18411311]

Europe PMC Funders Author Manuscripts

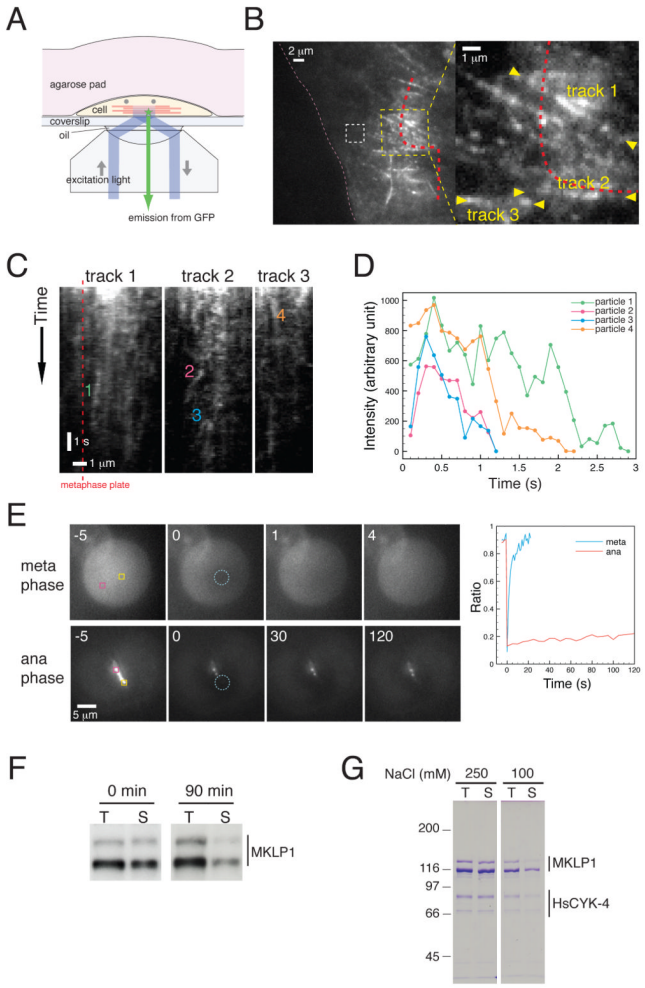

Figure 1.

Centralspindlin accumulates to the centre of the central spindle through clustering. (**A-E**) HeLa cells stably expressing functional HsCYK-4-GFP were observed by live imaging. (**A**) Schematic of the experimental setup used to observe the movement of HsCYK-4-GFP along the central spindle. (**B**) Image of a cell in early anaphase. The area in the left panel indicated by the yellow dotted square is shown magnified in the right panel. The plasma membrane is indicated with pink dotted lines. The position of metaphase plate (Figure S1) is indicated by a red dotted line. The white dotted square was used for background correction for fluorescence intensity in **D**. (**C**) Kymographs along microtubule tracks indicated in **B**. (**D**) Traces of the fluorescent intensity of the particles indicated in **C**. (**E**) HsCYK-4-GFP was photobleached in the areas indicated by dotted blue circles in cells in metaphase and anaphase. The ratio of the fluorescence signals in the bleached (yellow square) to the unbleached areas (magenta) was plotted. The time (sec) after photobleaching is shown. (**F**) Cell lysates were prepared from HeLa cells arrested at prometaphase (0 min) or 90 min after release from nocodazole. MKLP1 in total cell lysates (T) and in supernatants (S) following centrifugation was analysed by Western blotting. (**G**) Centralspindlin purified from HeLa cells in the presence of 250 mM NaCl was diluted into buffers containing the indicated concentration of salt. Proteins in total inputs (T) and supernatants (S) were detected by Coomassie staining after SDS-PAGE.

Europe PMC Funders Author Manuscripts

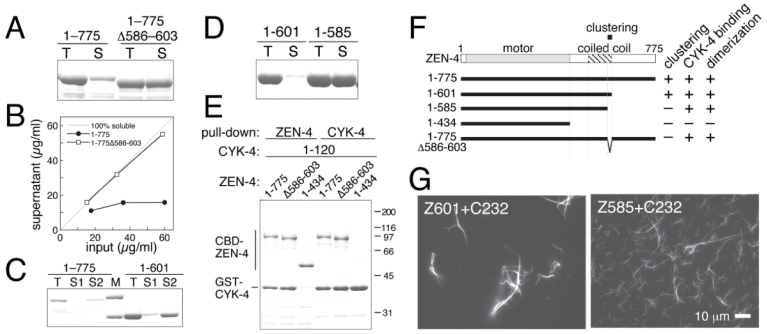

Figure 2.

In vitro characterization of the clustering of *C. elegans* centralspindlin. (**A-D**) Bacterially expressed ZEN-4 proteins were purified in the presence of 250 mM salt and diluted to (**A, B**) 150 mM or (**C, D**) 83 mM. Total input (T) and supernatant (S) after centrifugation were analysed by SDS-PAGE. For **C**, after the first supernatant (S1) was removed, the precipitate (not shown) was resuspended into a high salt buffer and centrifuged to obtain the second supernatant (S2). (**E**) CYK-4 binding was assayed by reciprocal pull-down from *E. coli* lysates expressing both ZEN-4 fragments tagged with chitin-binding domain (CBD) and CYK-4 1-120 tagged with glutathione S-transferase (GST). (**F**) Schematic model of ZEN-4 and deletion constructs used in this study with a summary of their in vitro properties. ZEN-4 is comprised of a motor domain, a neck region containing several helix-breaking proline residues, a 100 amino acid region that forms a parallel coiled coil [20] and a tail domain. A small region (‘clustering element’) is required for clustering. (**G**) Microtubule-bundling assays with ZEN-4 constructs competent (Z601) or incompetent (Z585) for clustering complexed with CYK-4 1-232 (C232).

Europe PMC Funders Author Manuscripts

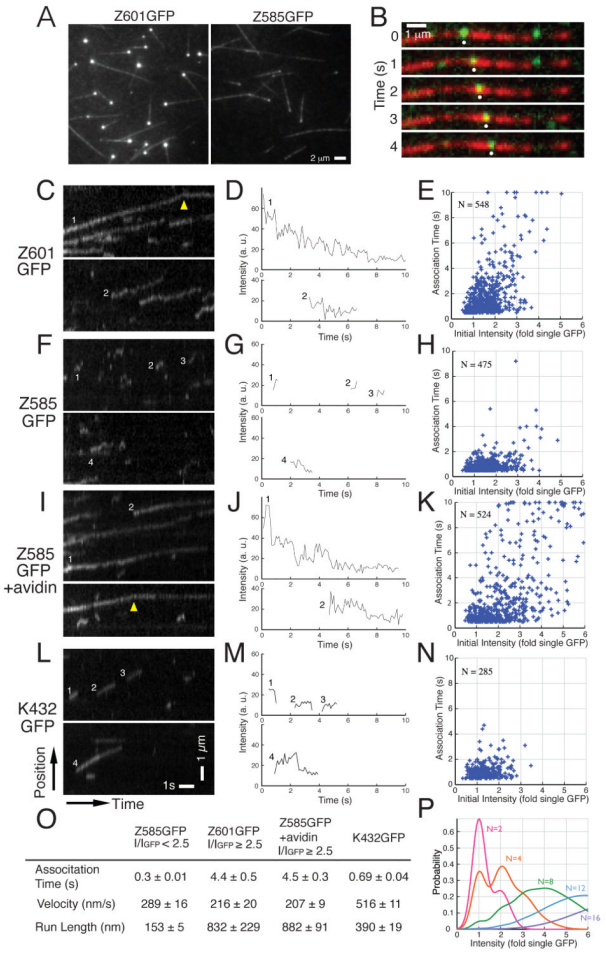

	Z585GFP I/IGFP < 2.5	Z601GFP I/IGFP ≥ 2.5	Z585GFP +avidin I/IGFP ≥ 2.5	K432GFP
Association Time (s)	0.3 ± 0.01	4.4 ± 0.5	4.5 ± 0.3	0.69 ± 0.04
Velocity (nm/s)	289 ± 16	216 ± 20	207 ± 9	516 ± 11
Run Length (nm)	153 ± 5	832 ± 229	882 ± 91	390 ± 19

Figure 3.

Clustering is essential for efficient transport of ZEN-4. (**A**) Still images from time-lapse observation of the interaction of Z601GFP or Z585GFP at 9 μg/ml with microtubules immobilized on a glass surface, showing plus-end accumulation of Z601GFP. (**B**) Frames from time-lapse observations showing a particle of Z601GFP (135 ng/ml, green) moving along a microtubule (red). White dot highlights a particle moving in a continuous manner. (**C, F, I, L**) Kymographs depicting the movement of indicated motor constructs along microtubules. Avidin induces clustering of Z585GFP that has a C-terminal biotin-tag (**I**). A dimeric Kinesin-1 construct (K432GFP) was also observed for comparison (**L-N**). The arrowhead in **C** and **I** indicates accumulation of particles at the plus-end of microtubule. (**D, G, J, M**) Traces of photobleaching behaviour of the particles in the corresponding kymographs. (**E, H, K, N**) Association time plotted against the initial fluorescence intensity of each particle. (**O**) Summary of association time, velocity and run length. (**P**) Simulation of distributions of fluorescence intensities of particles containing 2, 4, 8, 12, 16 GFP moieties, assuming 50% of GFPs are fluorescently active.

Europe PMC Funders Author Manuscripts

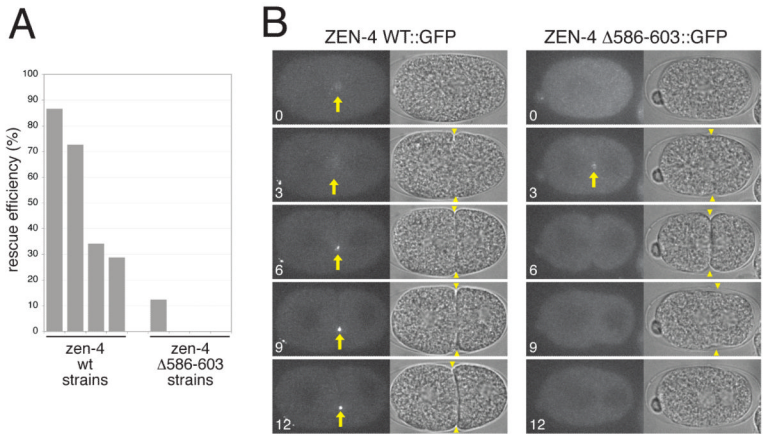

Figure 4.

Clustering of ZEN-4 is essential for cytokinesis. (**A**) Genetic analysis of the functionality of GFP-tagged wild-type (wt) and self-assembly incompetent (Δ586-603) *zen-4* transgenes. The mutant defective in clustering could barely rescue *zen-4* null animals to viability. (**B**) Time-lapse observation of the first cell division of the embryos from *zen-4* null hermaphrodite mothers rescued by wt or mutant transgenes. Wild-type ZEN-4 localizes to the central spindle and strongly accumulates to the midbodies (arrows). In contrast, the self-assembly incompetent mutant transiently associates with the central spindle and fails to accumulate to the midbody. The mutant embryos exhibited partial cleavage furrow ingression followed by regression (arrowheads), as seen for depletion of ZEN-4 by RNAi and is a consequence of centralspindlin-independent furrowing. Elapsed time is indicated in min.

Europe PMC Funders Author Manuscripts

Europe PMC Funders Author Manuscripts

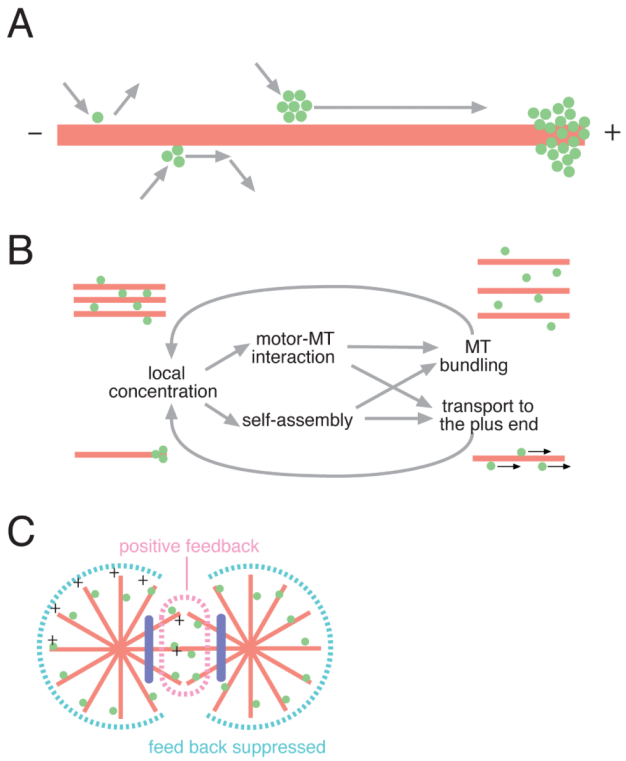

Figure 5.

(**A**) Schematic summarizing the effect of clustering of centralspindlin on its motility along microtubules. (**B**) Positive feedback loop model for the interaction between centralspindlin and microtubules. Red lines and green dots represent microtubules and the centralspindlin heterotetramers, respectively. (**C**) Model explaining how centralspindlin accumulates and bundles microtubules exclusively in the equatorial region of a normally dividing cell.